Prediction and classification of ventricular arrhythmia based on phase-space reconstruction and fuzzy c-means clustering

Hanjie Chen[a], Saptarshi Das[b,c], John M. Morgan[d] and Koushik Maharatna[a]

a) School of Electronics and Computer Science, University of Southampton, Southampton, SO17 1BJ, UK (hc4y15@soton.ac.uk, km3@ecs.soton.ac.uk)
b) Department of Mathematics, College of Engineering, Mathematics and Physical Sciences, University of Exeter, Penryn Campus, Penryn, TR10 9FE, UK (saptarshi.das@ieee.org, s.das3@exeter.ac.uk)
c) Institute for Data Science and Artificial Intelligence, University of Exeter, North Park Road, Exeter, Devon EX4 4QE, UK
d) Faculty of Medicine, University of Southampton, Tremona Road, Southampton, SO17 1BJ, UK (jmm@hrclinic.org)

Keywords: Ventricular Arrhythmia; Prediction and Classification; Phase Space Reconstruction; Fuzzy C-means Clustering

ABSTACT

Background and objective: Prediction and classification of Ventricular Arrhythmias (VA) may allow clinicians sufficient time to intervene for stopping its escalation to Sudden Cardiac Death (SCD). This paper proposes a novel method for predicting VA and classifying its type, in particular, the fatal VA even before the event occurs.

Methods: A statistical index *J* based on the combination of phase-space reconstruction (PSR) and box counting has been used to predict VA. The fuzzy c-means (FCM) clustering technique is applied for the classification of impending VA.

Results: 32 healthy and 32 arrhythmic subjects from two open databases; PTB Diagnostic database (PTBDB) and CU Ventricular Tachyarrhythmia (CUDB) database respectively; were used to validate our proposed method. Our method showed average prediction time of approximately 5 mins (4.97 mins) for impending VA in the tested dataset while classifying four types of VA (VA without ventricular premature beats (VPBs), ventricular fibrillation (VF), ventricular tachycardia (VT), and VT followed by VF) with an average 4 mins (approximately) before the VA onset, i.e., after 1 min of the prediction time point with average accuracy of 98.4%, a sensitivity of 97.5% and specificity of 99.1%.

Conclusions: The results obtained can be used in clinical practice after rigorous clinical trial to advance technologies such as implantable cardioverter defibrillator (ICD) that can help to preempt the occurrence of fatal ventricular arrhythmia - a main cause of SCD.

1. Introduction

Sudden Cardiac Death (SCD) remains a major cause of premature death in the developed world and is estimated to affect as many as 5 million people/year worldwide. The main reason behind the SCDs is fatal Ventricular Arrhythmia (VA) [1]. Typically, arrhythmias are detected using Electrocardiogram

(ECG) signals [2]. ECG by nature is a nonlinear and nonstationary signal. Therefore, it is prudent to treat ECG in its fundamental non-stationary form and apply signal processing methods such as, wavelet transform (WT) that can handle the inherent nonlinearity of an ECG signal [3]. Over the last two decades, different approaches based on ECG analysis for predicting arrhythmia have been explored, such as, VA prediction based on: Heart Rate Variability (HRV) [4, 5] and compression entropy from HRV parameters [6] that shows common patterns for impending VT. Also, empirical mode decomposition (EMD) [7], radial basis function neural network (RBFNN) [8], naive Bayes classifier [9] and artificial neural networks (ANN) [10] have been successfully applied for arrhythmia prediction. Apart from prediction, several methods have also been proposed for classifying VA such as, Support Vector Machines (SVM) [11, 12], thresholding method [13], random forest classifier [14], convolution neural networks (CNN) [15], C4.5 classifier [16], Markov model and morphology analysis [17], least square SVM classifier (LS-SVM) [18] and optimal orthogonal wavelet with SVM [19] etc.

However, the main emphasis of these existing works has been given on the prediction of non-fatal arrhythmias rather than the prediction of fatal arrhythmias. They can do successful classification of arrhythmias only after the actual event takes place. There is almost no literature that has taken a holistic view of both prediction and classification of arrhythmias before the actual event occurs [20]. Inspired by this fact, the aim of the present work is to develop a novel arrhythmia analysis methodology which not only can predict the impending fatal VA but is also capable of classifying the type of impending VA. Firstly, we firstly adapt a novel approach for identifying ECG features to predict the impending VA based on phase-space reconstruction (PSR) and box-counting techniques. Then a fuzzy c-means (FCM) clustering-based classifier is used to classify four different types of impending VA viz. VA without ventricular premature beats (VPBs), VT, VF and VT followed by VF.

The rest of the paper is organized as follows: in Section 2, we introduce the theoretical background of the PSR and FCM techniques. Then we describe our proposed algorithm in Section 3. The results and the discussion on the validation with PTBDB and CUDB are show in Section 4. Finally, conclusions and future work are drawn in Section 5.

2. Theoretical Background

The mechanism of the arrhythmias might be considered as a cumulative effect of atypical phase relationships between the electrical activities of the different chambers of heart leading to a chaotic desynchronization [20] in its overall operation. Had such desynchronization process been detected early, it could serve as a predictor of possible impending VA [20]. Phase-space reconstruction or time delay embedding method [21, 22] has widely been used in the field of nonlinear dynamics and nonlinear signal processing for detecting such desynchronization phenomena in a time-series data which is often indistinguishable even by expert human observations. Therefore, such technique when applied on ECG time-series may have potential for detecting the gradual phase desynchronization leading to the arrhythmia. Taking inspiration from our previous work [20] the present paper develops a new statistical index *J* for VA prediction based on PSR and box-counting technique and its performance was benchmarked with both healthy (from PTBDB) and arrhythmic subjects (from CUDB). First, we used PSR technique to plot the phase-space diagrams based on the ECG signals and its delayed versions. The number of trajectories from the phase-space diagram was quantified using box-counting method [20] in terms of number of black boxes which was used for formulating the risk index *J*. Once *J* reaches a

threshold indicating an impending VA event, the algorithm classifies the type of impending VA using FCM clustering technique based on the PSR features.

2.1. Phase Space Reconstruction and Box-counting

The PSR is a method to reconstruct the trajectory (phase space) of a system by plotting the original signal and its delayed versions [20]. It is widely applied to detect abnormal situations in a system of regular oscillations. Normally, the phase space of a system of fixed frequency oscillations within a limit cycle would be a closed contour. However, the trajectory will start to spread if the system becomes chaotic thereby filling the phase space [20]. In the healthy heart condition, within a small time window, the consecutive ECG beats can be considered as an almost quasi-periodic waveform [23]. Therefore, the phase-space analysis of it would produce an almost closed contour [24]. However, during arrhythmia episode, as the incoherent phase relationships between electrical activities of different chambers of heart lead the system toward chaos [20]. In this case, PSR method might be a good choice for arrhythmia analysis, since it can describe the phase space behavior of ECG signals to detect such a chaotic state and thereby helping to distinguish the normal and abnormal states of the heart. Recently, such technique has been widely applied in the field of ECG signal processing for heartbeat classification [25], ECG fiducial point detection [26], noise removal from ECG signal [27], fetal heart monitoring [28]. human identification [29] and arrhythmia classification [30].

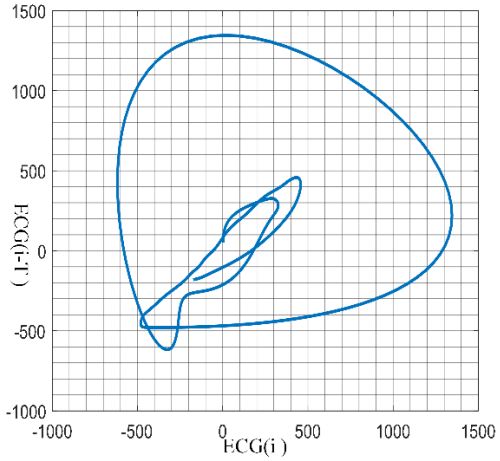

Fig.1: An example of box counting in phase-space diagram from healthy ECG signal (τ = 0.02s, N = 25).

Let us consider an ECG signal in one-dimension $x[i]$ and its delayed version $x[i-\tau]$, where $i = 1, 2, \cdots, N$, and N being the number of data-points and τ is the chosen time delay. Then the two-dimensional phase space diagram can be plotted with the x and y-axes representing the original and the delayed signal respectively. Following the exploration reported in [20], we choose 20 samples as an appropriate delay for the optimum PSR analysis of ECG signals with 1 KHz sampling frequency that gives good person-centric characterization. Then, the phase-space diagram can be divided into $N \times N$ pixels, where N is an integer. An example is given in Fig. 1. In this case, phase-space diagram of a normal ECG is plotted based on 0.02 seconds time delay (20 samples) and divided into 25×25 pixels. The pixels through which one or more trajectory pass are designated as black boxes (n_b) and others are considered as white boxes (n_w). The number of black boxes (n_b) reflects the spread of these trajectories [20] and thus can be considered as a feature to analyze the phase space diagram of ECG.

2.2. Fuzzy *c*-means clustering

The FCM clustering is a type of unsupervised machine learning algorithm that involves assigning all objects to different clusters, while objects belonging to the same cluster are as similar as possible. This technique has been applied recently for cardiac color ultrasound analysis [31], arrhythmia classification and detection [32, 33]; and detection of Premature Ventricular Contractions (PVCs) [34]. The FCM clustering technique is normally applied where each object may belong to more than one cluster. This is particularly important in our work as the subjects from VT followed by VF group contain the attributes from both VT and VF conditions and they possibly belong to more than one group. The FCM clustering is achieved based on the minimization of the objective function in (1) as:

$$FCM_m = \sum_{i=1}^{D}\sum_{j=1}^{N}\mu_{ij}^{m}\left\|x_i - c_j\right\|^2, \tag{1}$$

where, D is the number of objects and N is the number of clusters, m is the degree of fuzzy overlap, x_i and c_j represent the i^{th} object and the center of the j^{th} cluster respectively, μ_{ij} is the degree of membership of object x_i in the j^{th} cluster. Initially, the degree of cluster membership μ_{ij} is set randomly. Then the c_j and updated μ_{ij} are calculated by using formulas (2) and (3) respectively as:

$$c_j = \frac{\sum_{i=1}^{D}\mu_{ij}^{m}x_i}{\sum_{i=1}^{D}\mu_{ij}^{m}}, \tag{2}$$

and

$$\mu_{ij}^{m} = \frac{1}{\sum_{k=1}^{D}\left(\frac{\left\|x_i - c_j\right\|}{\left\|x_i - c_k\right\|}\right)^{\frac{2}{m-1}}}. \tag{3}$$

In our work, the number of objects D is 32, which is the number of the VA records we used. The number of clusters is 4 since four types of VA (VA without VPBs, VT, VF and VT followed by VF) is considered here. All objects x are firstly located in the co-ordinate system based on the calculated values of the *x*-axis and *y*-axis. For each object x_i (i = 1, 2, ⋯, 32), the center of each cluster c_j (j = 1, 2, ⋯, 4) will be calculated using (2) based on a random cluster membership μ_{ij}. Then, repeating to calculate the c_j with updated μ_{ij} and objective function FCM_m until the FCM_m improves by less than a minimum threshold or after a maximum number of iterations. The sum of the cluster membership values μ_{ij} should be 1, where lower value represents the object is unlikely to belong to this cluster, higher value means the object is more likely member of that cluster. The detailed description will be given in Section 3.2.

3. Methodology

Since ECG by nature is a nonlinear and nonstationary signal, in this work, we treated ECG in its fundamental non-stationary form and applied signal processing methods that can handle its inherent non-linearity and non-stationarity. The block diagram of the proposed system for VA prediction and classification has been shown in Fig. 2. The prediction system consists of four stages in Fig. 2a. The first stage includes fourth order Butterworth high-pass filter and low-pass filter with cut-off frequency of 1 Hz and 30 Hz respectively to remove ECG baseline wandering and measurement noise [35]. Then, the filtered signals were normalized using equation (4) to ensure all data lies in the range of [0, 1]. In the second stage, the phase space diagram of a healthy ECG template and its corresponding number of black boxes are determined using the PSR and box-counting techniques. The number of black boxes for the healthy template was used as the standard to compare abnormal ECG cases. In this work, the time delay for PSR is 20 samples and the value of N for box-counting is 2^{10}, which are the same as the previous work [20]. After that, we choose a sliding window of 5 seconds of ECG signals with 4 seconds overlap for the ECG segment before the onset of VA condition and applied PSR and box-counting technique to

determine the number of black boxes for each time window. Finally, the risk index *J* is calculated based on the difference of the number of black boxes between each sliding time window and the healthy template. For classification system in Fig. 2b, it includes two main steps. Firstly, once the risk index reaches the threshold, we extract features based on the number of black boxes and the risk index during next few seconds. Secondly, the FCM clustering technique is used to classify four different types of VA. The data normalization is given as:

$$\tilde{x}(t) = (x(t) - x_{min})/(x_{max} - x_{min}). \quad (4)$$

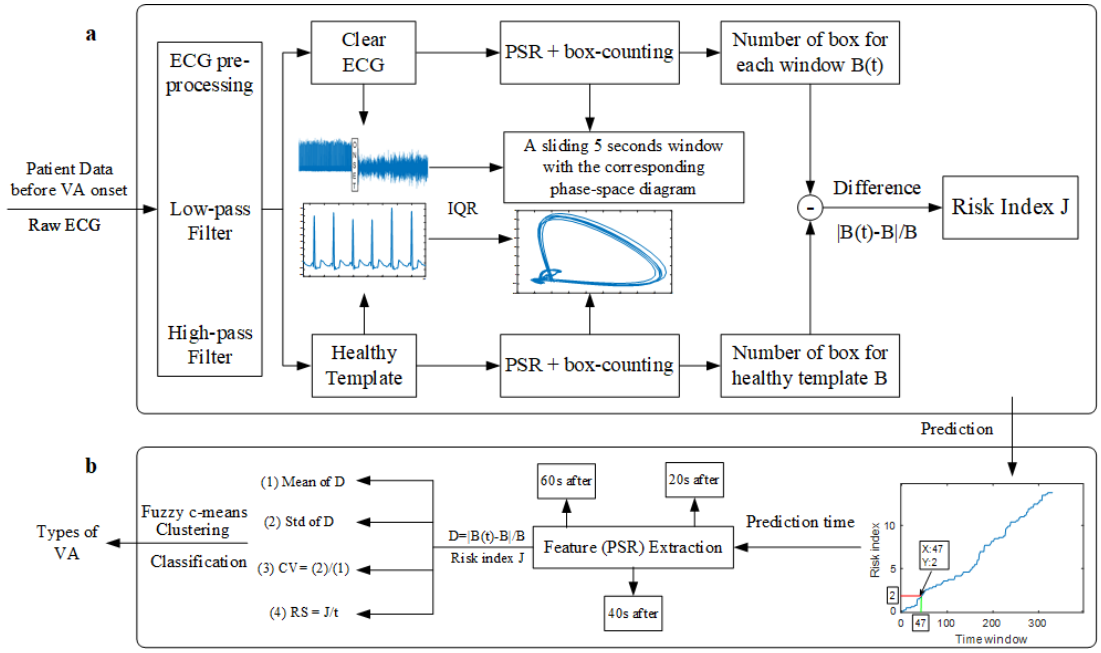

Fig.2: System overview of both VA prediction and classification. **a**, Prediction of VA using PSR and box-counting. **b**, Classification of VA based on PSR features using fuzzy *c*-means clustering technique.

3.1. Formulation of the Prediction Index for Impending VA

First, mean of the number of the black boxes from the healthy template (B_{mean}) for each individual ECG record is calculated. Then we developed the risk index *J* based on this value to predict VA. We obtained the number of black boxes for all consecutive 5 seconds of time windows with 4 seconds overlap before the VA ($B(t)$). They were divided into four categories based on the difference between $B(t)$ and B_{mean} ($\left|\frac{B(t)-B_{mean}}{B_{mean}}\right|$), which are normal and three abnormal cases. We found for most of the healthy subjects, the values of $\left|\frac{B(t)-B_{mean}}{B_{mean}}\right|$ are less than 10%. Therefore, we decided to use 10% as a threshold to distinguish between the normal and abnormal situations - if the difference between $B(t)$ and B_{mean} is less than 10% of B_{mean}, the ECG signals in that time window is then considered as a normal case. For abnormal cases, there are three different levels when the difference between $B(t)$ and B_{mean} is larger than 10% of B_{mean}, which are 10% to 15%; 15% to 20% and larger than 20% respectively. Subsequently, the *J* is generated based on these situations, and formulated as (5):

$$J(t) = \begin{cases} X(t) & t = 1 \\ J(t-1) + X(t) & 1 < t < n, \end{cases} \quad (5)$$

where, *n* is the number of the time windows, $X(t)$ is the index value of the t^{th} time window, which can be divided into five different situations as shown in (6):

$$X(t)=\begin{cases} 0, & \left|\frac{B(t)-B_{mean}}{B_{mean}}\right| \le 10\% \\ \omega_1, & 10\% < \left|\frac{B(t)-B_{mean}}{B_{mean}}\right| \le 15\% \\ \omega_2, & 15\% < \left|\frac{B(t)-B_{mean}}{B_{mean}}\right| \le 20\% \\ \omega_3, & 20\% < \left|\frac{B(t)-B_{mean}}{B_{mean}}\right| \\ -0.1, & \left|\frac{B(t)-B_{mean}}{B_{mean}}\right| \le 5\%(\boldsymbol{condition_1}). \end{cases} \quad (6)$$

Here, $B(t)$ is the number of the black boxes in the t^{th} time window and B_{mean} is the mean of the number of black boxes for the healthy template. As mentioned earlier, if the difference between $B(t)$ and B_{mean} is less than 10%, that time window is considered as a normal situation and the index value $X(t)$ is zero. Among three abnormal situations, ω_1, ω_2 and ω_3 represent the index value of the t^{th} time window when$\left|\frac{B(t)-B_{mean}}{B_{mean}}\right|$), are between 10% and 15%, between 15% and 20% and larger than 20% respectively. In this case, ω_1, ω_2 and ω_3 are the weighting factors and their sum should be one [20]. The weighting factors determine the contributions of these three abnormal situations toward the final risk index J for impending VA and the larger the value of $\left|\frac{B(t)-B_{mean}}{B_{mean}}\right|$, larger the weighting factor. In our work, we chose three different combinations of ω_1, ω_2 and ω_3 with (0.6,0.25,0.15); (0.5,0.3,0.2) and (0.4,0.35,0.25) and finally chose 0.5, 0.3 and 0.2 as the ω_1, ω_2 and ω_3 respectively, since this combination gave us the most obvious difference of J between the three groups (healthy, VA without VPBs and VA with VPBs), as shown in Table 1. In order to avoid the situation of progressively increasing of J, we have set a condition (**condition 1** in (6)) to reduce it. This condition should be stricter than the condition of normal window. Therefore, we set 5% as a threshold to signify the completely normal ECG, leading to the reduction of J index. In this case, if the values of $\left|\frac{B(t)-B_{mean}}{B_{mean}}\right|$ in ten successive time windows are lower than 5%, the trend of ECG is considered to become completely normal. In this case, J reduces to 0.1 and the minimum value of J is zero.

Table 1. The average values of J in each group based on three different combinations of weight

Group	The combination of weight to calculate J		
(ω_1, ω_2, ω_3)	(0.6,0.25,0.15)	(0.5,0.3,0.2)	(0.4,0.35,0.25)
Healthy	0.1688	0.1375	0.1425
VA without VPBs	4.525	4.875	4.675
VA with VPBs	38.57	46.18	41.82

3.2. Classification of VA

Once the risk index reaches the threshold, an impending VA situation is considered. In order to understand the regularity of continuous ECG time windows after the prediction time and classify the VA before its onset, we have extracted the ECG PSR features during the next 20, 40 and 60 seconds and compared the performance based on the corresponding accuracy. These features are extracted based on the $\left|\frac{B(t)-B_{mean}}{B_{mean}}\right|$ and risk index J by calculating the mean (μ), standard deviation (σ), coefficient variation (CV) and rising speed (RS) as shown in equation (7):

$$\begin{cases} \mu = mean\left(\left|\frac{B(t)-B_{mean}}{B_{mean}}\right|\right), CV = \sigma/\mu, \\ \sigma = \sqrt{(\left|\frac{B(t)-B_{mean}}{B_{mean}}\right| - \mu)^2}, RS = J/t. \end{cases} \quad (7)$$

All subjects from four different classes are assigned into four clusters by using the FCM clustering. All subjects are displaced into a two-dimension coordinate system with their RS - (X axis) and CV - (Y axis). The degrees of membership of each subject for four clusters are calculated based on the distance between itself and the center of each cluster. Finally, the cluster with the highest degree of membership is

recognized as the group of the corresponding subject. As mentioned above, the subjects from VT followed by VF group contain the features from both VT and VF conditions and they possibly belong to more than one group. Therefore, the choice of degree of fuzzy overlap is important in our work. In this case, the number of the cluster N is 4 since we have four different types of VA and the degree of fuzzy overlap m is generally chosen as 2 [36]. We also identify the subjects that their highest cluster membership value is smaller than 0.6 as the fuzzy overlaps, since these subjects possibly belong to more than two clusters. The whole operation will stop once the number of iterations reaches a maximum of 20 or the improvement of the objective function is less than 0.001 between the final two iterations.

4. Results and Discussions

4.1. Description of the ECG Data

The proposed system was evaluated using the publicly available ECG databases from PhysioNet [37]. In this paper, 32 subjects both from PTBDB (Lead I) [38] and CUDB [39] were used to analyze both the healthy and arrhythmic ECG conditions respectively. The ECG signals from the PTBDB were sampled at 1 KHz whereas, the CUDB signals were originally sampled at 250 Hz. To bring them to a uniform platform we interpolated the CUDB signals to 1 KHz. Here, we only used 32 subjects in CUDB, since other 3 records from CUDB *CU*21*m*, *CU*33*m* and *CU*35*m* have large amount of artefacts before the VA onset. Hence it is difficult to extract features for VA prediction. For these arrhythmic subjects, we analyzed the ECG segment that precedes the onset of the VA condition. The ECG signals after the VA onset are not used in our work.

4.2. Prediction of VA

Among 32 healthy subjects in PTBDB, the maximum value J attained was 1.4 with its value for most of the subjects (22 subjects) remaining at zero and others in Fig. 3(**a**). The 32 arrhythmic subjects from the CUDB were divided into four groups, which are VA without VPBs, VT, VF and VT followed by VF. The values of J based on the three different combinations of weighting factor are shown in Fig. 3(**b**). The combination of the weighting factors ω_1, ω_2 and ω_3 (refer to the methodology section) with 0.5, 0.3 and 0.2 respectively gave us the most obvious difference of J between three groups (healthy, VA without VPBs and VA with VPBs). Hence, we chose this combination to calculate J. The comparison results of J between healthy subjects in PTBDB and arrhythmic subjects in CUDB is done based on the healthy template - in essence, a 5s segments is taken from the healthy part of ECG in subject-specific way - as shown in Table 2. It shows the risk index J for most of the healthy subjects in PTBDB are zero and the highest value of all healthy subjects is 1.4 while, the lowest value of J for all arrhythmic subjects (except *CU*30*m*) in CUDB are greater than 2. Here, the information of subject *CU*30*m* is not available, since there are insufficient ECG data before VA onset to calculate the risk index. Therefore, according to our analysis, the condition $J > 2$ might signify an impending VA. The time point, where J reaches to 2 is recorded as prediction time point. Another interesting point to note is that for the VA without VPBs group (*CU*01*m*, *CU*06*m*, *CU*07*m*, *CU*28*m*), J is relatively lower than the other three groups. This is due to the fact that immediately after the occurrence of a VPB, the value of J increases significantly.

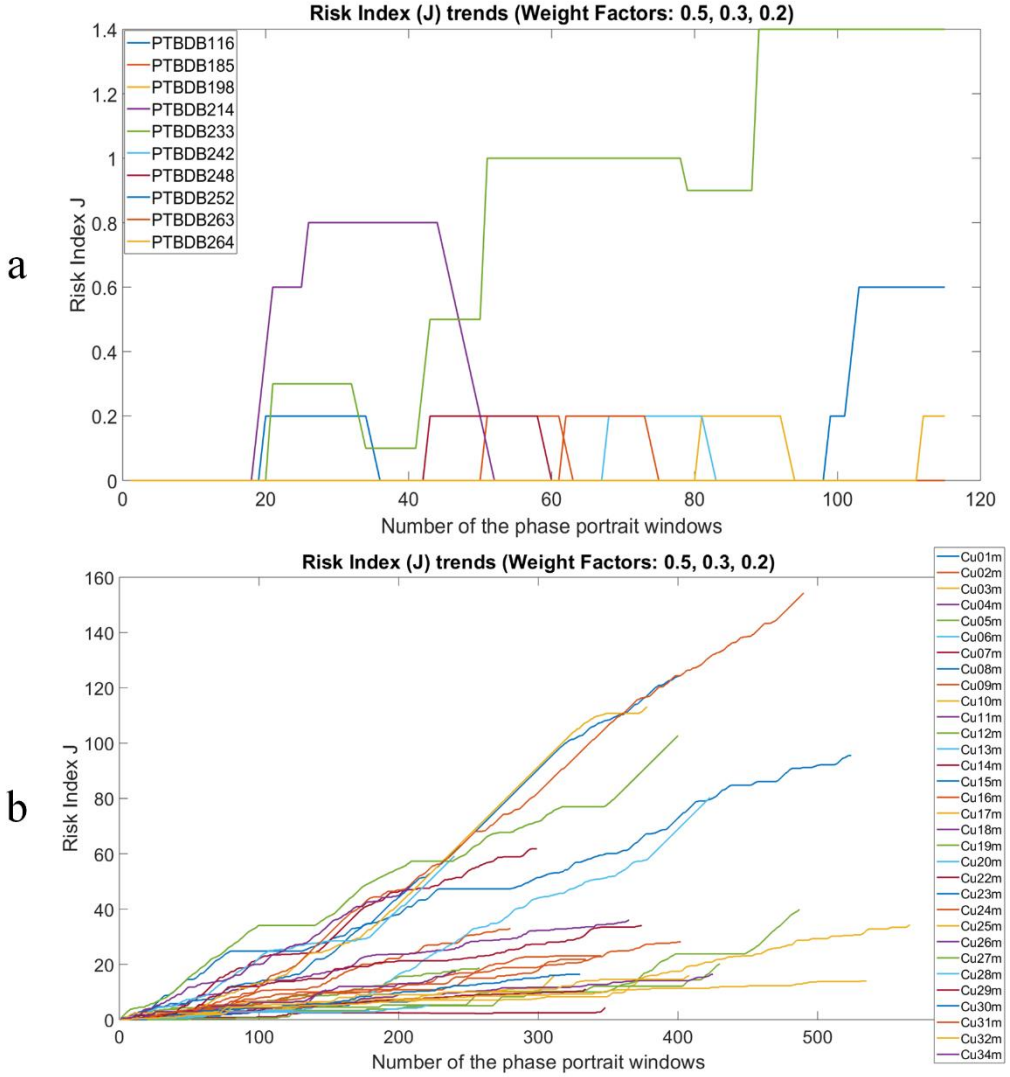

Fig.3: The risk index *J* trends. **a**: Results of 10 healthy subjects in PTBDB. **b:** Results of 32 arrhythmic subjects in CUDB.

4.3. Classification of VA

The classification of VA is achieved based on the PSR features using FCM clustering technique. The main reason of choosing FCM clustering to classify VA is that this method can identify data points, that potentially belong to multiple clusters (groups). In CUDB, the subjects from VT followed by VF group may have the same or similar features as VT or VF groups making them candidate of multiple groups. In our work, we extracted the ECG PSR features during the 20, 40 and 60 seconds after the prediction time point for each subject in order to evaluate the accuracy of the classifier employed and classification time before the VA onset. The average values of CV and RS of *J* for four types of VA was calculated using (7) with 95% confidence interval and are shown in Table 3. It is apparent that there is significant variation in terms of CV and RS for the four different types of VA and therefore these parameters were used for the classification purpose. The performance of VA classification based on the different features using FCM clustering are shown in Fig. 4. The classification performance is better if the average maximum value is closer to 1. The results based on 20 seconds (top) and 40 seconds (middle) PSR features after prediction time point show two and one fuzzy overlaps respectively. The result based on

60 seconds (bottom) PSR features after prediction time point shows no fuzzy overlap with the highest average maximum value of 0.927. Here the advantage of FCM clustering showed that we can simply see the number of overlaps based on the time length of PSR features. With 60 seconds PSR features, all groups are directly clustered without overlap and hence we decided to use 60 seconds PSR features to classify VA.

Table 2. The highest risk index *J* for both healthy and arrhythmic subjects in PTBDB and CUDB (N/A: not available)

Class of Database	Patient ID in PTBDB	Highest *J*	Class of Database	Patient ID in CUDB	Highest *J*
Healthy Subjects	PTB105	0	VA without VPBs	CU01m	6.8
	PTB116	0.2		CU06m	3.3
	PTB117	0		CU07m	4.4
	PTB122	0		CU28m	5
	PTB155	0		CU30m	N/A
	PTB156	0	VF	CU08m	102.7
	PTB166	0		CU11m	154.3
	PTB170	0		CU22m	113.1
	PTB180	0		CU23m	124.2
	PTB182	0	VT	CU02m	33
	PTB185	0.2		CU04m	10.9
	PTB198	0.2		CU05m	20.2
	PTB214	0.8		CU13m	16.2
	PTB229	0		CU16m	23.1
	PTB233	1.4		CU17m	11
	PTB235	0		CU20m	59.2
	PTB236	0		CU25m	15.9
	PTB237	0		CU26m	17.3
	PTB238	0		CU27m	34.1
	PTB240	0		CU31m	36.1
	PTB242	0.2		CU32m	14
	PTB244	0		CU34m	48.2
	PTB246	0	VT followed by VF	CU03m	34.4
	PTB247	0		CU09m	21.8
	PTB248	0.2		CU10m	95.5
	PTB251	0		CU12m	18.6
	PTB252	0.6		CU14m	61.8
	PTB155	0		CU15m	16.4
	PTB260	0		CU18m	16.4
	PTB263	0.2		CU19m	39.9
	PTB264	0.2		CU24m	28.1
	PTB266	0		CU29m	80.4

Table 3. The feature extraction of all subjects based on CV and RS

Parameters	VA without VPBs	VF	VT	VT followed by VF
Average CV	1.100	0.549	0.321	0.761
Average RS	0.034	0.329	0.109	0.191
CV interval (95% CI)	(0.99, 1.21)	(0.48, 0.59)	(0.19, 0.44)	(0.54, 0.94)
RS interval (95% CI)	(0.02, 0.04)	(0.29, 0.39)	(0.08, 0.15)	(0.14, 0.29)

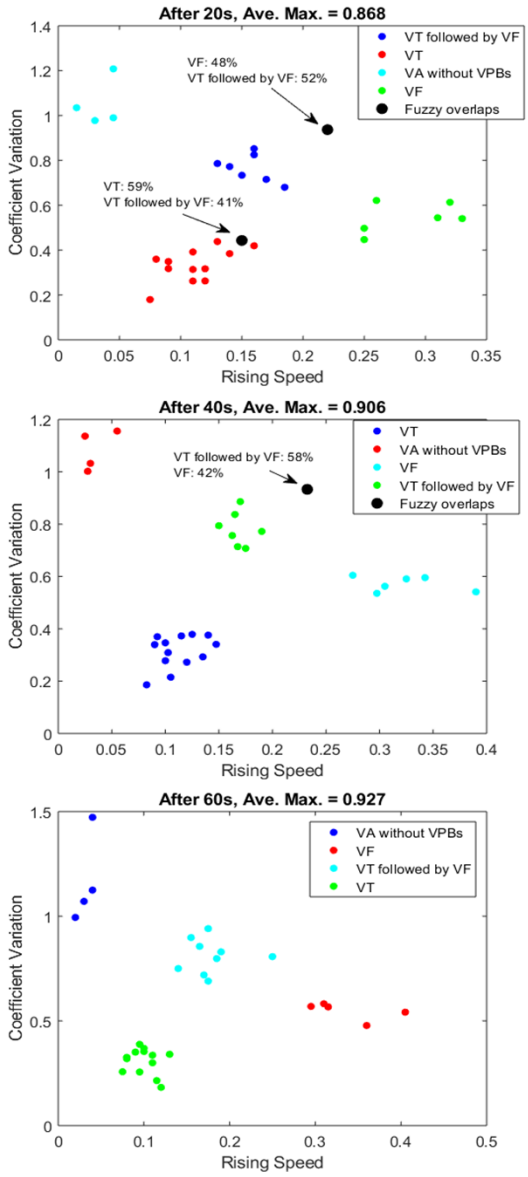

Fig.4: The classification results based on different length of ECG features after the prediction time point.

Their average classification time before VA onset and the corresponding accuracy are shown in Fig. 5. The result based on 20s and 40s PSR features after prediction time point shows the same accuracy of 93.5% with two and one fuzzy overlap respectively. The best result was obtained using 60s PSR features after prediction time point with 96.8% accuracy and no fuzzy overlap. Hence, we have selected to use the features during 60s after the prediction time for each subject. Fig. 6 (**top**) and Fig. 6 (**bottom**) shows the confusion matrix and ROC of VA classification respectively. Among 31 subjects (except *CU*30*m*), the sensitivity of VF group is 80%, since one subject from the other group is recognized as VF group. The specificity of VT followed by VF is 90%, because one subject from this group is considered as VF group. Concerning ROC figure, the middle gray line means random guess, the classification performance is better when ROC is closer to 1. From our results, the ROC of all the four VA groups is close signifying high performance for VA classification.

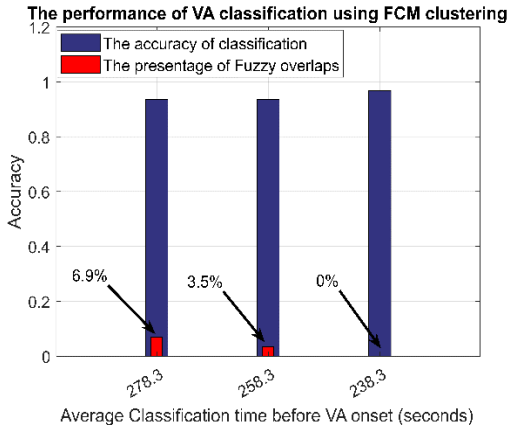

Fig.5: The performance of VA classification with average classification time before VA onset.

Fig.6: The confusion matrix of VA classification (top), The ROC of VA classification (bottom).

4.4. Evaluation of the Method

For prediction of VA, we evaluate our method by computing the prediction time - defined as the time point where $J > 2$ before the arrhythmia onset - for each arrhythmic subject in CUDB and compare the results to the previous works [20] which is shown in Table 4. The average prediction time for all subjects is 4.97 mins, which is 50 seconds earlier than the previous work [20], with the best and the worst-case prediction time being 8.68 mins (*CU*03*m*) and 1.78 mins (*CU*06*m*) respectively. Our results show that the prediction time for different subject varies widely since it is relative to the length of the analyzed ECG data before the VA onset. Here, we provided the correlation between the length of the healthy ECG

data before the VA onset (analysis time) and the corresponding prediction time for each of the subjects in Fig. 7. It shows that all the data points can be fitted around a straight line with the correlation coefficient R = 0.952. This result clearly shows that there is a strong positive linear relationship between the prediction times and the length of the data that was available for analysis before the VA onset. Hence it implies that if we can have longer length of analysis with data before VA onset, the performance of our prediction method will be even better; a scenario that can be satisfied for long-term ECG monitoring either by conventional ECG systems at the hospitals or through wearable ECG sensors in a nomadic environment.

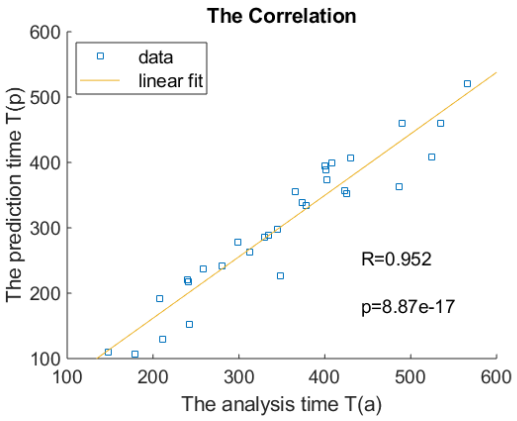

Fig. 7: The correlation between the length of the analyzed ECG data before VA onset $T(a)$ and prediction time before VA onset $T(p)$.

In order to evaluate the performance of VA prediction, we used a leave one out cross-validation (LOOCV) method to calculate the true positive (TP), true negative (TN), false positive (FP) and false negative (FN) with positive P (VA subjects) and negative N (Healthy subjects). Here, we derived the prediction performance based on sensitivity (SE), specificity (SP), accuracy (ACC), positive predictive value (PPV), negative predictive value (NPV), false positive rate (FPR), false discovery rate (FDR), false negative rate (FNR) and F_1 score using the following formulas in (8):

$$\begin{cases} \mathrm{SE} = \frac{\mathrm{TP}}{\mathrm{P}} = \frac{\mathrm{TP}}{\mathrm{TP+FN}}, & \mathrm{SP} = \frac{\mathrm{TN}}{\mathrm{N}} = \frac{\mathrm{TN}}{\mathrm{FP+TN}}, & \mathrm{ACC} = \frac{\mathrm{TP+TN}}{\mathrm{P+N}}, \\ \mathrm{PPV} = \frac{\mathrm{TP}}{\mathrm{TP+FP}}, & \mathrm{NPV} = \frac{\mathrm{TN}}{\mathrm{TN+FN}}, & \mathrm{FPR} = \frac{\mathrm{FP}}{\mathrm{N}} = \frac{\mathrm{FP}}{\mathrm{FP+TN}}, \\ \mathrm{FDR} = \frac{\mathrm{FP}}{\mathrm{FP+TP}}, & \mathrm{FNR} = \frac{\mathrm{FN}}{\mathrm{FN+TP}}, & \mathrm{F_1\ score} = \frac{2\mathrm{TP}}{2\mathrm{TP+FP+FN}}. \end{cases} \tag{8}$$

The Table 5 depicts the comparison of prediction measures between the previous work [20] and our work using LOOCV approach which shows that with the proposed risk index J, we obtained 100% SE, ACC, NPV and F_1 score, which are better than the previous work [20].

Table 4. The comparison of prediction time between the previous work and our work (N/A: not available)
(Prediction time: The time length between prediction time point and VA onset)

Class of Database	Patient ID in CUDB	Time before VA onset (s)	Prediction time of Previous work (s) [20]	Prediction time of our work (s)
VA without VPBs	CU01m	211	34.3	130
	CU06m	179	21.9	107
	CU07m	348	195.1	227
	CU28m	221	97.2	152
	CU30m	N/A	14.6	N/A
VF	CU08m	524	135.7	408
	CU11m	490	359.3	460
	CU22m	378	336.7	334
	CU23m	401	323.3	389
VT	CU02m	280	172	242
	CU04m	148	107.5	110
	CU05m	430	358.7	407
	CU13m	312	343.4	263
	CU16m	345	222.2	297
	CU17m	334	520.5	289
	CU20m	240	197.5	220
	CU25m	408	360.8	399
	CU26m	241	70.1	217
	CU27m	400	213	395
	CU31m	365	250.8	355
	CU32m	535	381.6	460
	CU34m	208	122.3	192
VT followed by VF	CU03m	566	413.5	521
	CU09m	334	214.4	288
	CU10m	423	294.4	357
	CU12m	258	200	237
	CU14m	299	242	278
	CU15m	401	323.2	389
	CU18m	425	329.3	352
	CU19m	487	422.1	363
	CU24m	402	337.5	374
	CU29m	374	321.9	339
	Average	351.4	245.2	298.3

Table 5. The comparison of prediction performance between the previous work and our work under a LOOCV scheme

Prediction measures (%)	Previous work [20]	Our work
SE	96.88	100
SP	100	100
ACC	98.44	100
PPV	100	100
NPV	96.97	100
FPR	0	0
FDR	0	0
FNR	3.13	0
$F_1\ score$	98.41	100

In addition, the classification measures of each type of VA are calculated using (8) and the results are shown in Table 6. Our methodology achieved an average sensitivity, specificity and accuracy of 97.5%, 99.1% and 98.4% respectively for VA classification. Among 31 subjects (except *CU*30*m*), only one of the subjects with VT followed by VF group was recognized as VF group. However, since subject from VT followed by VF group finally goes to the VF condition, it is logical to consider them as VF group in which case the classification performance goes to 100%. We also compared our technique to other previously established algorithms that were mentioned in the literature.

Table 6. The classification performance of our system for VA classification

Classification Measures (%)	VA without VPBs	VF	VT	VT followed by VF	Average
SE	100	100	100	90	97.5
SP	100	96.3	100	100	99.1
ACC	100	96.8	100	96.8	98.4
PPV	100	80	100	100	95
NPV	100	100	100	95.5	98.9
FPR	0	3.7	0	0	0.93
FDR	0	20	0	0	5
FNR	0	0	0	10	2.5
$F_1\ score$	100	88.9	100	94.7	95.9

Table 7. The classification performance of VA classification in other literature (N/A: Not Available)

Authors	Method Used	Classifier	Arrhythmia classes	Performance (%)
Li *et al.* [11]	14 different features	SVM classifier	VF and VT	Acc:96.3, SE:98.4, SP:98
Alonso-Atienza *et al.* [12]	Time-frequency parameters	SVM classifier	Shockable and non-shockable (VF, VT)	Acc:96, SE:92, SP:97
Roopaei *et al.* [13]	Chaotic features	Thresholding	VF and VT	Acc: 88.6
Tripathy *et al.* [14]	Entropy features	Random forest classifier	Shockable and non-shockable (VF, VT)	Acc:97.23, SE:96.54, SP:97.97
Acharya *et al.* [15]	Time segments	Convolution neural network	Shockable and non-shockable (VF, VT)	Acc:93.18, SE:95.32, SP:91.04
Mohanty *et al.* [16]	Hybrid features	C4.5 classifier	VF, VT and NSR	Acc:97.02, SE:90.97, SP:97.86
Gawde *et al.* [17]	Probabilistic transition graph	Markov model	VF and VT	SE:96.15, SP:93.5
Tripathy *et al.* [18]	Magnitude-phase features	LS-SVM classifier	VF and VT	Acc:94.32, SE:92.48, SP:95.53
Sharma *et al.* [19]	Entropy features	SVM classifier	Shockable and non-shockable (VF, VT)	Acc:97.8, SE:93.45, SP:98.35
Our proposed method	Phase-space features	Fuzzy c-means Clustering	VF, VT, and VT followed by VF	Acc:98.4, SE:97.5, SP:99.1

The comparison results are given in Table 7. Li *et al.* [11] suggested to use 14 different features for each 5 seconds time windows and combined with SVM to classify VT and VF with 96.3% accuracy, 98.4% sensitivity and 98% Specificity. Similarly, Alonso-Atienza *et al.* [12] showed the same classifier with time-frequency features to classify shockable and non-shockable VT and VF with an average accuracy of 96%. Roopaei *et al.* [13] have evaluated chaotic features based on the PSR of ECG to classify VT and VF using a threshold-based approach. However, the performance of their algorithm is 88.6% accuracy, which is lower than the other methods. Tripathy *et al.* [14] and Acharya *et al.* [15] represented two simple

algorithms to classify shockable and non-shockable VT and VF. Tripathy *et al.* [14] developed a random forest classifier with entropy features with 97.23% accuracy. Acharya *et al.* [15] designed a CNN classifier and combined with time features, the accuracy of their method is 93.18%. Mohanty *et al.* [16] presented a novel C4.5 classifier based on statistical, temporal and spectral features to classify normal ECG, VT and VF with 97.02% of accuracy. We have also compared the performance of our method with some algorithms from recently published studies like [17, 18, 19]. It is noted that these three algorithms are all consisted of a simple classifier and a novel feature extraction approach. Gawde *et al.* [17] proposed a method to classify VT and VF with 96.15% sensitivity and 93.5% specificity by identifying subset of Markov models of VA sub-classes based on probabilistic transition graph features. Tripathy *et al.* [18] introduced digital Taylor-Fourier transform to extract magnitude and phase features of ECG signals. Then LS-SVM classifier were applied based on these features and achieved an average accuracy of 94.32% to classify VT and VF. Sharma *et al.* [19] developed a simple SVM method to classify shockable and non-shockable VT and VF with 97.8% accuracy. The Fuzzy and Renyi entropy features were extracted using the optimal orthogonal wavelet filter to train the SVM classifier. Overall, it is evident that our proposed method has comparable or better performance than the previous methods for VA classification. The algorithm in [11] has the higher sensitivity than our method. However, it can only classify two types of VA, also the accuracy of this algorithm is lower than our work. Besides, our method shows the added advantage that here the classification is possible even before the event actually occurs.

5. Conclusion and future work

This paper studies prediction and classification of fatal VA using phase-space reconstruction and fuzzy *c*-means clustering and subsequently, a risk index has been proposed. The number of black box based on the trajectory of the ECG phase-space diagrams was calculated using the box-counting technique and the difference of the number of black-boxes between subject-specific normal ECG template and a sliding window of 5 seconds of the ECG signal is used to formulate a prediction risk index *J*. Then we use FCM clustering to classify four different types of ventricular arrhythmias based on phase-space features. However, we only used 64 ECG records to evaluate our proposed method as a proof-of-concept study. In the future, the proposed method may be evaluated based on larger sample size. In addition, the 3-dimensional phase space diagram can be further applied to extract more useful features of ECG to improve the prediction of VA [40]. As a conclusion, the major findings of the proposed method are that for the first time it has been shown that it is not only possible to predict an impending arrhythmia sufficiently before its actual occurrence in time but also is possible to classify the type of arrhythmia before it actually occurs (1 min after the prediction time point). We believe this is a novel result over existing approaches that can be used in clinical practice after rigorous clinical trial to advance technologies such as implantable cardioverter defibrillator (ICD) that can help to preempt the occurrence of fatal ventricular arrhythmia - a main cause of SCD.

References

[1] Z. Szabo, D. Ujvarosy, T. Ötvös, V. Sebestyén, and P. P.Nanasi, “Handling of ventricular fibrillation in the emergency setting,” *Frontiers in Pharmacology*, vol. 10, p.1640, 2020.

[2] H. Chen, K. Maharatna, An automatic R and T peak detection method based on the combination of hierarchical clustering and discrete wavelet transform, *IEEE Journal of Biomedical and Health Informatics* vol. 24, no. 10 pp. 2825–2832, 2020.

[3] S.Aziz, S. Ahmed and S. M. Alouini "ECG-based machine-learning algorithms for heartbeat classification," *Scientific Reports* , vol. 11, no. 1, pp. 1-14, 2021.

[4] N. Wessel, C. Ziehmann, J. Kurths, U. Meyerfeldt, A. Schirdewan, and A. Voss, "Short-term forecasting of life-threatening cardiac arrhythmias based on symbolic dynamics and finite-time growth rates," *Physical Review E*, vol. 61, no. 1, p. 733, 2000.

[5] M. J. Reed, C. Robertson, and P. Addison, "Heart rate variability measurements and the prediction of ventricular arrhythmias," *QJM*, vol. 98, no. 2, pp. 87–95, 2005.

[6] M. Baumert, V. Baier, J. Haueisen, N. Wessel, U. Meyerfeldt, A. Schirdewan, and A. Voss, "Forecasting of life threatening arrhythmias using the compression entropy of heart rate," *Methods of Information in Medicine*, vol. 43, no. 02, pp. 202–206, 2004.

[7] A. Riasi and M. Mohebbi, "Predicting imminent episodes of ventricular tachyarrhythmia using an entropy-based feature in the emd domain," in *2015 23rd Iranian Conference on Electrical Engineering*. IEEE, 2015, pp. 88–92.

[8] J. Kelwade and S. Salankar, "Radial basis function neural network for prediction of cardiac arrhythmias based on heart rate time series," in *2016 IEEE First International Conference on Control, Measurement and Instrumentation (CMI)*. IEEE, 2016, pp. 454–458.

[9] N. Bayasi, T. Tekeste, H. Saleh, B. Mohammad, A. Khandoker, and M. Ismail, "Low-power ECG-based processor for predicting ventricular arrhythmia," *IEEE Transactions on Very Large Scale Integration (VLSI) Systems*, vol. 24, no. 5, pp. 1962–1974, 2015.

[10] E. R. Adams and A. Choi, "Using neural networks to predict cardiac arrhythmias," in *2012 IEEE International Conference on Systems, Man, and Cybernetics (SMC)*. IEEE, 2012, pp. 402–407.

[11] Q. Li, C. Rajagopalan, and G. D. Clifford, "Ventricular fibrillation and tachycardia classification using a machine learning approach," *IEEE Transactions on Biomedical Engineering*, vol. 61, no. 6, pp. 1607– 1613, 2013.

[12] F. Alonso-Atienza, E. Morgado, L. Fernandez-Martinez, A. García- Alberola, and J. L. Rojo-Alvarez, "Detection of life-threatening arrhythmias using feature selection and support vector machines," *IEEE Transactions on Biomedical Engineering*, vol. 61, no. 3, pp. 832–840, 2013.

[13] M. Roopaei, R. Boostani, R. R. Sarvestani, M. A. Taghavi, and Z. Azimifar, "Chaotic based reconstructed phase space features for detecting ventricular fibrillation," *Biomedical Signal Processing and Control*, vol. 5, no. 4, pp. 318–327, 2010.

[14] R. Tripathy, L. Sharma, and S. Dandapat, "Detection of shockable ventricular arrhythmia using variational mode decomposition," *Journal of Medical Systems*, vol. 40, no. 4, p. 79, 2016.

[15] U. R. Acharya, H. Fujita, S. L. Oh, U. Raghavendra, J. H. Tan, M. Adam, A. Gertych, and Y. Hagiwara, "Automated identification of shockable and non-shockable life-threatening ventricular arrhythmias using convolutional neural network," *Future Generation Computer Systems*, vol. 79, pp. 952–959, 2018.

[16] M. Mohanty, S. Sahoo, P. Biswal, and S. Sabut, "Efficient classification of ventricular arrhythmias using feature selection and c4. 5 classifier," *Biomedical Signal Processing and Control*, vol. 44, pp. 200–208, 2018.

[17] P. R. Gawde, A. K. Bansal, and J. A. Nielson, "Integrating Markov model and morphology analysis for finer classification of ventricular arrhythmia in real time," in *2017 IEEE EMBS International Conference on Biomedical & Health Informatics (BHI)*. IEEE, 2017, pp. 409–412.

[18] R. K. Tripathy, A. Zamora-Mendez, J. A. De la O Serna, M. R. A. Paternina, J. G. Arrieta, and G. R. Naik, "Detection of life threatening ventricular arrhythmia using digital Taylor Fourier transform," *Frontiers in Physiology*, vol. 9, p. 722, 2018.

[19] M. Sharma, R.-S. Tan, and U. R. Acharya, "Detection of shockable ventricular arrhythmia using optimal orthogonal wavelet filters," *Neural Computing and Applications*, vol. 32, no. 20, pp. 15869–15 884, 2020.

[20] G. Cappiello, S. Das, E. B. Mazomenos, K. Maharatna, G. Koulaouzidis, J. Morgan, and P. E. Puddu, "A statistical index for early diagnosis of ventricular arrhythmia from the trend analysis of ECG phase-portraits," *Physiological Measurement*, vol. 36, no. 1, p. 107, 2014.

[21] H. Kantz and T. Schreiber. "Nonlinear time series analysis," *Cambridge University Press*, vol. 7. 2004.

[22] M. Small "Applied nonlinear time series analysis: applications in physics, physiology and finance," *World Scientific*. vol. 52. 2005.

[23] G. Chakraborty, T. Kamiyama, H. Takahashi and T. Kinoshita ''An efficient anomaly detection in quasi-periodic time series data—a case study with ECG," *International Work-Conference on Time Series Analysis*. Springer, Cham, pp. 147-157, 2017

[24] O. Fojt and J. Holcik, "Applying nonlinear dynamics to ECG signal processing," *IEEE Engineering in Medicine and Biology Magazine*, vol. 17, no. 2, pp. 96-101, 1998.

[25] I. Nejadgholi, M. H. Moradi, and F. Abdolali, "Using phase space reconstruction for patient independent heartbeat classification in comparison with some benchmark methods," *Computers in Biology and Medicine*, vol. 41, no. 6, pp. 411–419, 2011.

[26] Z. Hou, Y. Dong, J. Xiang, X. Li, and B. Yang, "A real-time QRS detection method based on phase portraits and box-scoring calculation," *IEEE Sensors Journal*, vol. 18, no. 9, pp. 3694–3702, 2018.

[27] J.-W. Lee, K.-S. Kim, B. Lee, B. Lee, and M.-H. Lee, "A real time QRS detection using delay-coordinate mapping for the microcontroller implementation," *Annals of Biomedical Engineering*, vol. 30, no. 9, pp. 1140–1151, 2002.

[28] Z. Wei, L. Hongxing, and C. Jianchun, "Adaptive filtering in phase space for foetal electrocardiogram estimation from an abdominal electrocardiogram signal and a thoracic electrocardiogram signal," *IET Signal Processing*, vol. 6, no. 3, pp. 171–177, 2012.

[29] S.-C. Fang and H.-L. Chan, "Human identification by quantifying similarity and dissimilarity in electrocardiogram phase space," *Pattern Recognition*, vol. 42, no. 9, pp. 1824–1831, 2009.

[30] H. Chen, S. Das, J. Morgan, K. Maharatna, "An effective PSR-based arrhythmia classifier using self-similarity analysis", *Biomedical Signal Processing and Control*, vol. 69, pp. 102851, 2021.

[31] J. Dongdong, N. Arunkumar, Z. Wenyu, L. Beibei, Z. Xinlei, and Z. Guangjian, "Semantic clustering fuzzy c means spectral model based comparative analysis of cardiac color ultrasound and electrocardiogram in patients with left ventricular heart failure and cardiomyopathy," *Future Generation Computer Systems*, vol. 92, pp. 324–328, 2019.

[32] N. A. H. Haldar, F. A. Khan, A. Ali, and H. Abbas, "Arrhythmia classification using Mahalanobis distance based improved fuzzy *c*-means clustering for mobile health monitoring systems," *Neurocomputing*, vol. 220, pp. 221–235, 2017.

[33] C. Roopa, B. Harish, and S. A. Kumar, "A novel method of clustering ECG arrhythmia data using robust spatial kernel fuzzy *c*-means," *Procedia computer science*, vol. 143, pp. 133–140, 2018.

[34] R. Gharieb, M. Massoud, S. Nady, and M. Moness, “Fuzzy *c*-means in features space of teager-kaiser energy of continuous wavelet coefficients for detection of PVC beats in ECG,” in *2016 8th Cairo International Biomedical Engineering Conference (CIBEC)*. IEEE, 2016, pp. 72–75.
[35] A. Amann, R. Tratnig, and K. Unterkofler, “Reliability of old and new ventricular fibrillation detection algorithms for automated external defibrillators,” *Biomedical Engineering Online*, vol. 4, no. 1, p. 60, 2005.
[36] O. Kesemen, Ö. Tezel, and E. Özkul, “Fuzzy *c*-means clustering algorithm for directional data (fcm4dd),” *Expert Systems with Applications*, vol. 58, pp. 76–82, 2016.
[37] A. L. Goldberger, L. A. Amaral, L. Glass, J. M. Hausdorff, P. C. Ivanov, R. G. Mark, J. E. Mietus, G. B. Moody, C.-K. Peng, and H. E. Stanley, “Physiobank, physiotoolkit, and physionet: components of a new research resource for complex physiologic signals,” *Circulation*, vol. 101, no. 23, pp. e215–e220, 2000.
[38] R. Bousseljot, D. Kreiseler, and A. Schnabel, “Nutzung der ekgsignaldatenbank cardiodat der ptb über das internet,” *Biomedizinische Technik/Biomedical Engineering*, vol. 40, no. s1, pp. 317–318, 1995.
[39] F. Nolle, F. Badura, J. Catlett, R. Bowser, and M. Sketch, “Crei-gard, a new concept in computerized arrhythmia monitoring systems,” *Computers in Cardiology*, vol. 13, pp. 515–518, 1986.
[40] M. Nandi, J. Venton, and P. J. Aston, “A novel method to quantify arterial pulse waveform morphology: attractor reconstruction for physiologists and clinicians,” *Physiological Measurement*, vol. 39, no. 10, p. 104008, 2018.